Steel and Composite Structures, Vol. 13, No. 1 (2012) 15-33
DOI: http://dx.doi.org/10.12989/scs.2012.13.1.015

Ultimate capacity of welded box section columns with slender plate elements

Hong-Xia Shen*

School of Civil Engineering, Xi'an University of Architecture and Technology, Xi' an 710055, PR China

(Received May 30, 2011, Revised February 20, 2012, Accepted April 02, 2012)

Abstract. For an axially loaded box-shaped member, the width-to-thickness ratio of the plate elements preferably should not be greater than 40 for Q235 steel grades in accordance with the Chinese code GB50017-2003. However, in practical engineering the plate width-to-thickness ratio is up to 120, much more than the limiting value. In this paper, a 3D nonlinear finite element model is developed that accounts for both geometrical imperfections and residual stresses and the ultimate capacity of welded built-up box columns, with larger width-to-thickness ratios of 60, 70, 80, and 100, is simulated. At the same time, the interaction buckling strength of these members is determined using the effective width method recommended in the Chinese code GB50018-2002, Eurocode 3 EN1993-1 and American standard ANSI/AISC 360-10 and the direct strength method developed in recent years. The studies show that the finite element model proposed can simulate the behavior of nonlinear buckling of axially loaded box-shaped members very well. The width-to-thickness ratio of the plate elements in welded box section columns can be enlarged up to 100 for Q235 steel grades. Good agreements are observed between the results obtained from the FEM and direct strength method. The modified direct strength method provides a better estimation of the column strength compared to the direct strength method over the full range of plate width-to-thickness ratio. The Chinese code and Eurocode 3 are overly conservative prediction of column capacity while the American standard provides a better prediction and is slightly conservative for $b/t = 60$. Therefore, it is suggested that the modified direct strength method should be adopted when revising the Chinese code.

Keywords: width-to-thickness ratio; welded box-shaped section; axially loaded members; ultimate capacity; direct strength method; effective width method; FEM.

1. Introduction

For an axially loaded member, a thin-walled wide profile, which is liable to achieve equal stabilities for both x and y axes, should be preferred, and a typical one is the welded square box section. This kind of cross section has been used in Beijing national stadium, and the width-to-thickness ratios of its plate elements exceed 40 which is the upper limit value to guard against local buckling for Q235 steel as recommended in the Code for design of steel structures GB50017-2003, some of which even attain 120 (Fan *et al.* 2006).

For axially compressed members with the width-to-thickness ratio of the plate element exceeding the limit value, plate local buckling may occur before the overall buckling. However, local buckling of plates does not mean the loss of member's load carrying capacity owing to the post-buckling strength of the buckled plates.

* Corresponding author, Associate Professor, E-mail: shenhongxia88@126.com

Some researches have been conducted for welded box section columns. Usami and Fukumoto (1982, 1984) conducted experiments to investigate the local and overall interaction buckling strength of welded built-up box compression members. Guo(1992) studied the post-buckling behavior and ultimate strength of the welded thin-walled box-section and I-section stub columns under combined loading of axial compression and bending at the ends using spline finite strip method. Pircher *et al.* (2002) investigated the influence of the imperfections induced during the fabrication process on the buckling of thin-walled steel box sections by a finite element analysis, and a modified Winter formula for predicting the ultimate strength of a plate was proposed. Degée *et al.* (2008) examined the interaction of global and local buckling in welded RHS compression members taking account of the residual stresses due to welding and local as well as global geometrical defects by experimental and numerical investigations, and a new definition of the column slenderness together with the use of buckling curve *a*, instead of curve *b* as recommended by current EN 1993-1, was used to design the thin-walled box columns to consider the interaction between local and global stability failure.

Although several studies have been made on the welded box sections, further work is still needed. For now, no design formula was given (Guo 1992), and design method based upon an effective width concept was proposed (Usami and Fukumoto 1982, Usami and Fukumoto 1984, Guo 1992, Pircher *et al.* 2002, Degée *et al.* 2008). Moreover, technical Codes, such as GB50018-2002, Eurocode 3 and ANSI/AISC 360-10, are also based on the effective width method. The effective width method is a useful design model, but it has some shortcomings (Schafer 2008, Rusch *et al.* 2001), in particular the calculation of complex effective section properties. In order to do this, sometimes cumbersome iterations are required. Therefore, in recent years, a simpler method, i.e., the direct strength method, was developed by Schafer and Peköz (Rusch *et al.* 2001). Also it was proved to be effective in predicting the strength of cold-formed steel members (Schafer 2008, Rusch *et al.* 2001, Sputo *et al.* 2005, Tovar *et al.* 2005, Yu *et al.* 2007, Becque *et al.* 2008, de Miranda Batista 2009 and Zhu *et al.* 2006), and formally adopted in North American cold-formed steel design specifications in 2004 as an alternative to the traditional effective width method. It is well known that the welded section members contain higher residual stresses and exhibit larger plastic deformation when subjected to loading compared to the cold-formed section members. Although Kwon *et al.* (2007) investigated the ultimate strength and performance of the welded H and channel section columns undergoing nonlinear interaction between local and overall buckling and confirmed that direct strength formulas in AISI Supplement 2004 that had been modified could properly predict the ultimate strength of welded H and channel section columns when local and flexural buckling occur simultaneously, whether it is also applicable to the welded box sections or not is not known. To fulfill this need, the study presented in this paper develops a finite element model by using ANSYS program (Swanson Analysis Systems Inc 2004) and the ultimate capacity of axially loaded welded box section members, with slender plate elements, is modeled. Further, the numerical results are compared with those calculated by the effective width method adopted in GB50018-2002, ANSI/AISC 360-10 and Eurocode 3 and direct strength method in AISI 2004 so as to evaluate the applicability of the two methods.

2. Geometric model

2.1 Research object

Research object of this paper focuses on a pin-ended steel member subjected to axial load, with

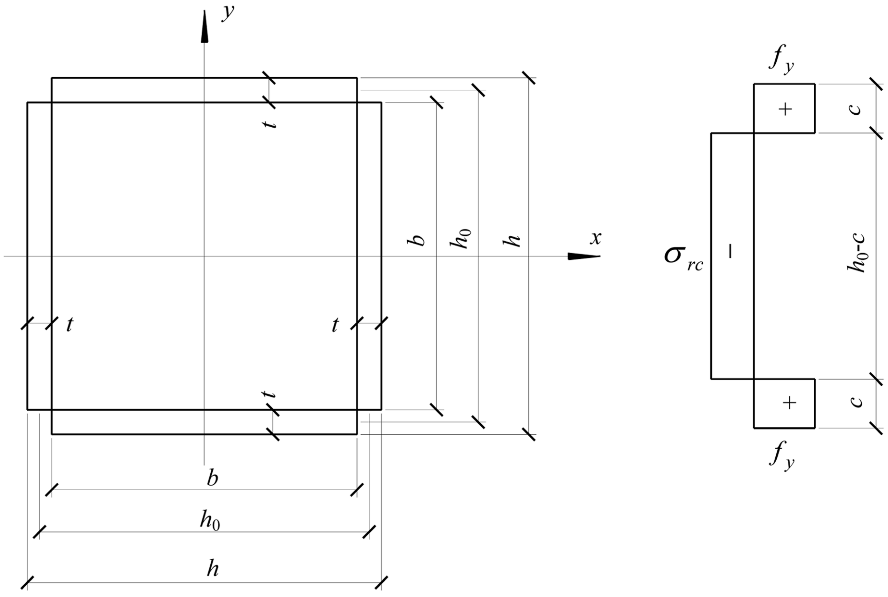

(a) (b)

Fig. 1 Welded box-shaped section (a) Geometric dimension (b) Residual stress distribution

square box section fabricated from slender plates welded together at the corners. The geometric dimensions of the cross-section are shown in Fig. 1(a). The box-shaped sections with large plate width-to-thickness ratios of 60, 70, 80, and 100 are investigated in which both geometrical and material nonlinearities are taken into consideration.

2.2 Initial imperfection

Two types of initial imperfections, namely residual stresses and initial curvatures, are taken into account. Because of the similar residual stress distributions on four plates of the cross-section, only one of them is plotted in simplified pattern (Chen 1992) in Fig. 1(b), where tensile residual stresses are designated as positive and compressive stresses as negative. Tensile residual stresses near the weld, with a magnitude equal to the yield strength, f_y, extend over a width of $c = 3t$, t is the thickness of the plate. According to the equilibrium condition, the magnitude of compressive residual stresses is equal to

$$\sigma_{rc} = \frac{2_c}{h_0 - 2c} f_y \tag{1}$$

where h_0 is the distance between the centre lines of the two opposite plates (see Fig. 1(a)).

Both the global and local initial deflections are taken into account. The global initial curvature is taken as a half-wave sine curve with an amplitude of $l/1000$, where l is the length of a column. Due to the similarity of the four plate elements, no interaction exists between the two adjacent plates and any of them may be regarded as simply supported at its four edges. Thus, making use of a coordinate system shown in Fig. 1(a), the forms of local initial deflections are assumed as follows

$$\omega = \omega_0 \sin\frac{m\pi z}{l}\cos\frac{\pi x}{b} \quad (y = \pm h_0/2) \tag{2a}$$

$$\text{or } \omega = \omega_0 \sin\frac{m\pi z}{l}\cos\frac{\pi y}{b} \quad (x = \pm h_0/2) \tag{2b}$$

where b is the plate width; $m = l/b$, which is the buckling half-wave number along the axial direction (z–direction) of a member; the magnitude of initial imperfection ω_0 in local mode is taken as $b/100$ and $b/1000$.

3. Finite element model and verification

Besides test, numerical simulation (i.e., finite strip method and FEM) has proved to be very useful and effective in predicting the strength of cold-formed steel members (Schafer 2008, Rusch *et al.* 2001, Sputo *et al.* 2005, Tovar *et al.* 2005, Yu *et al.* 2007, Becque *et al.* 2008, Becque *et al.* 2009). In this study, the FEM is used for welded sections.

3.1 Element type

If the maximum carrying-capacity of a regular column were investigated, the best element type would be a beam element (e.g., Beam189), which can reduce the number of computational elements, thus saving time. However, for a column with large plate width-to-thickness ratio, the influence of local buckling need to be considered and a shell element should be the choice. In this study, Shell181 element (Swanson Analysis Systems Inc 2004) is employed.

3.2 Material model

A rate-independent plasticity model is adopted to simulate the inelastic behavior of the steel. Von

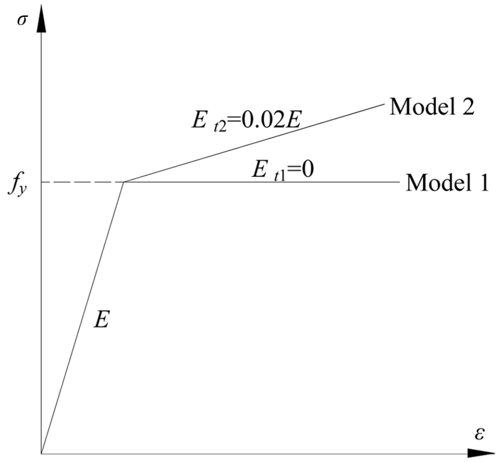

Fig. 2 Stress-strain curve for steel

Fig. 3 Initial geometric imperfections imposed by direct modelling

Mises yield criterion is used to define the material yield surface, and an associated flow rule to determine the plastic deformation in ANSYS program (Swanson Analysis Systems Inc 2004). A bilinear kinematic hardening model as shown in Fig. 2 is taken to simulate the elastic and inelastic behavior of steel, where the Young's modulus $E = 206{,}000$ MPa, Poisson's ratio $v = 0.3$, yield strength of the steel $f_y = 235$ MPa, and the tangent modulus E_t after yielding is taken as 0 and 0.02 E (i.e. 4120 MPa).

3.3 Direct modelling method

For the purpose of taking account of geometric imperfections, i.e., global and local initial deflections, direct modelling method is used. The number of nodes required and the order in which they should be generated are determined firstly,and then all nodes are generated according to the x, y, and z coordinates considering geometric imperfections. Further, the element attributes (element type, material, and real constant) having been set, shell elements are automatically generated within each area defined by four nodes. For any plate in a box section column, element size is $h_0/8$ along its width and $h_0/4$ in longitudinal direction, and thus the grid is $h_0/8 \times h_0/4$. In this study, the minimum grid is approximately 20 mm × 40 mm and the maximum one 50 mm × 100 mm, which satisfies the accuracy requirement. Fig. 3 shows the initial geometric imperfections imposed by direct modelling, in which the initial deflections are enlarged 5000 times in order to observe clearly.

3.4 Load application

Residual stress can be treated as initial stress, which is a loading and must be specified at all integration points of shell elements in ANSYS software (Swanson Analysis Systems Inc 2004). For a shell element, there are four integration points in its plane, together with 5 integration points in the thickness direction to take account of nonlinear bending properties, and thus the total number of integration points is 20. In order to apply initial stress, two steps must be carried out. Firstly, an initial stress file need to be written based on the integration point locations, and secondly the initial stress file must be read by using the ISFILE command only in the first load step of an analysis, as required in ANSYS program (Swanson Analysis Systems Inc 2004). In this study, because of thin plate elements, the same residual stress distributions along the thickness direction are assumed.

An end plate with a thickness of 30 mm is attached to both ends of a member. According to the plane cross-section assumption, that is, a cross-section does not deform in its own plane and remains a plane after flexural deformation, three translations in x, y, and z directions, at all nodes located on the same straight line parallel to the x axis, are coupled together respectively to make them have a same displacement along any direction, as shown in Fig. 4(b) with the master nodes lying at the center. The columns are assumed to be pin-ended, which means that the rotations around x and y axes (i.e., flexural deformations) are allowed and the rotation around z axis (i.e., torsional deformation), on the contrary, is not. In this paper, only the rotation around x axis is permitted. Therefore, the boundary conditions are defined as follows (Fig. 4(a))

when $z = 0$	$U_x = U_y = 0$	(for all master nodes)
	$U_z = 0$	(for the master node on the neutral axis)
when $z = l$	$U_x = U_y = 0$	(for all master nodes)

where U_x, U_y and U_z are x-, y- and z-translations. Besides, a lateral bracing is provided at mid-span, by specifying $U_x = 0$ at four corner nodes of the cross-section, to prevent the flexural buckling about y axis. In order to ensure stable and fast convergence, as well as obtain the descending branch of the load-deformation curve, displacement loading is adopted, in which a large displacement along the z direction, for example $U_z = -100$ mm, is applied at the master node coinciding with the coordinate origin at $z = l$. Fig. 4 is a typical finite element model built according to the above method.

3.5 Verification of the finite element model

In order to verify the finite element model mentioned above, a total of twenty-one experimental

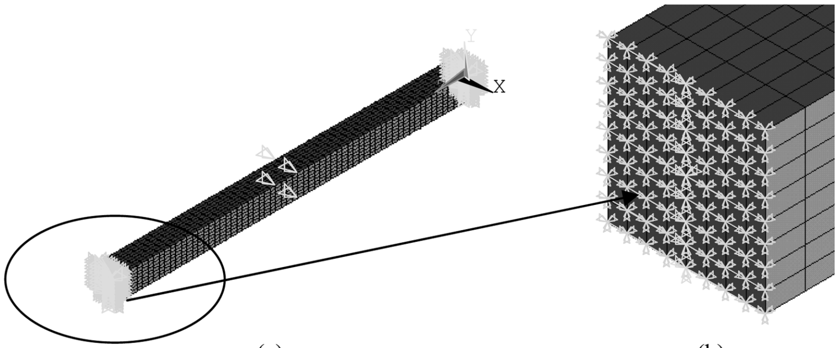

Fig. 4 Typical finite element model (a) Shell element model (b) End boundary conditions

Table 1 Comparison between the numerical and experimental results (Usami and Fukumoto 1982, 1984)

Specimen	φ_1	φ_2	$\frac{\varphi_2 - \varphi_1}{\varphi_1} \times 100$ (%)	Specimen	φ_1	φ_2	$\frac{\varphi_2 - \varphi_1}{\varphi_1} \times 100$ (%)
S-35-22	0.852	0.829	−2.72	R-50-44	0.579	0.589	1.73
S-35-33	0.722	0.732	1.32	R-65-22	0.593	0.594	0.17
S-35-38	0.621	0.626	0.78	R-65-27	0.637	0.574	−9.82
S-35-44	0.544	0.549	0.88	R-65-33	0.585	0.613	4.79
S-50-22	0.740	0.694	−6.24	R-40-29	0.798	0.770	−3.51
S-50-27	0.672	0.684	1.72	R-40-44	0.644	0.651	1.09
S-50-33	0.670	0.708	5.63	R-40-58	0.498	0.484	−2.85
R-50-22	0.743	0.687	−7.48	R-65-29	0.619	0.654	5.69
R-50-27	0.731	0.678	−7.28	R-65-44	0.521	0.533	2.42
R-50-33	0.709	0.699	−1.41	R-65-58	0.441	0.462	4.86
R-50-38	0.639	0.687	7.50				

specimens which were centrally loaded (Usami and Fukumoto 1982, 1984) are analyzed firstly. Material properties, residual stresses, and initial deflections as measured (Usami and Fukumoto 1982, 1984) are adopted. The numerical results are listed in Table 1. "S" refers to the specimens having square box sections, and "R" the specimens having rectangular box sections. The number following S and R is the value of slenderness ratio, and the last number is the value of width-to-thickness ratio of the flange plates. In Table 1, φ_1 and φ_2 represent the stability factors obtained from experiment and FEM analysis. Comparison shows that the numerical results agree very well with the experimental results, indicating that the finite element model provided in this study can accurately predict the local and overall interaction buckling strength of welded box columns.

4. Analysis of the numerical results

Five different sizes of cross-sections with the width-to-thickness ratios (b/t) of 40, 60, 70, 80, and 100 are simulated. For every section, the slenderness ratio, $l = l/r$ (r is the radius of gyration of the cross-section about the buckling axis), is taken as 40, 50, 60… 140, 160, 180, and 200. The following is an analysis of the computed results.

4.1 The effect of different parameters on the compressive behavior of welded box columns

4.1.1 Material model

Two material models $E_{t1} = 0$ and $E_{t2} = 0.02\,E$, as shown in Fig. 2, are used to calculate the ultimate capacity of welded box columns with $b/t = 40$, and the numerical results are plotted in Fig. 5 and the ultimate capacities, P_{u1} and P_{u2}, are listed and compared in Table 2. In Fig. 5, the abscissa represents the compression deformation along the column length, denoted by U_z in mm, and the ordinate the load carrying capacity in kN. As seen in Fig. 5, except for the short columns, the material model has almost no influence on the compressive behavior of welded box columns. For a short column, model 2 with strain hardening has much more strength reserve after the maximum value than model 1 with the slope 0. Along with the increase in the column length, this difference becomes less and less. For a long

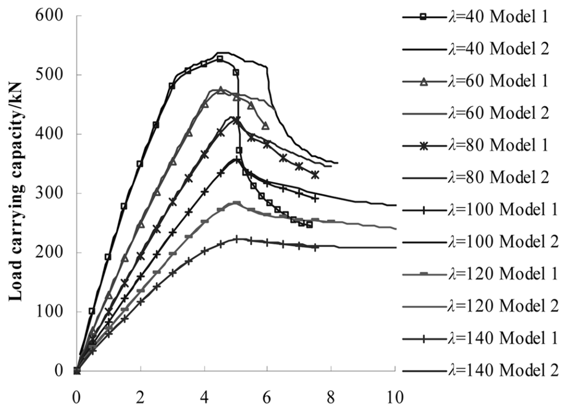

Fig. 5 Effect of material model

Table 2 Comparison between the maximum numerical results with material model 1 and 2

λ	P_{u1}/kN	P_{u2}/kN	P_{u2}/P_{u1}
40	526.07	537.59	1.022
50	498.99	508.05	1.018
60	486.68	474.53	0.975
70	460.35	454.37	0.987
80	422.23	428.03	1.014
90	395.5	394.67	0.998
100	357.84	357.65	0.999
110	318.55	318.85	1.001
120	283.32	283.61	1.001
130	252.14	252.2	1.000
140	222.98	222.84	0.999
150	198.53	198.74	1.001
	Average value		1.001

column, the numerical results with model 1 coincide with those with model 2. Also the comparison between the maximum numerical results in Table 2 shows that the calculation results are very close with two material models, and the slope 0 or 0.02 E in strain-hardening zone has no influence on the ultimate load carrying capacity. Therefore, elastic-perfectly plastic is assumed and material model 1 $E_{t1} = 0$ is used in the further study.

4.1.2 Magnitude of initial imperfection in local mode

The amplitude value of ω_0 in local mode is taken as $b/100$ and $b/1000$ respectively to exam the influence of local imperfection on the interaction buckling behavior of box section columns with

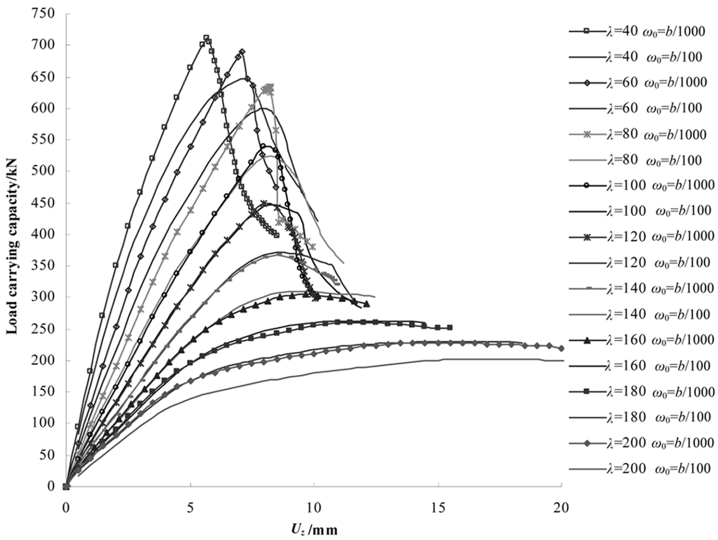

Fig. 6 Effect of amplitude of local imperfection

Table 3 Comparison between the maximum numerical results with different magnitudes of local imperfection

λ	the maximum capacities P_{u3} (kN) $\omega_0 = b/100$	the maximum capacities P_{u4} (kN) $\omega_0 = b/1000$	P_{u4}/P_{u3}
40	646.83	710.76	1.099
60	599.81	689.78	1.150
80	522.30	633.57	1.213
100	447.81	539.05	1.204
120	372.00	448.13	1.205
140	309.36	368.04	1.190
160	262.89	304.97	1.160
180	229.56	260.28	1.134
200	202.40	228.11	1.127
	Average value		1.165

$b/t = 60$. The load carrying capacity-compression deformation curves are shown in Fig. 6 and the maximum numerical results are listed in Table 3. It can be seen that the large difference exists between the numerical results with different amplitudes and that the compressive behavior of welded box columns is very sensitive to local imperfections. Therefore, it is very important to define properly the magnitude of initial imperfection in local mode. Although the magnitude of initial imperfection in local mode is not specified uniformly, and it was taken as 0.01 (Kwon *et al*. 2007), $b/1000$ (Degée *et al*. 2008) and $l/10000$ (Yang *et al*. 2007), it is proved that the value of $b/1000$ seems to be reasonable in several literatures (for example, Degée *et al*. 2008) when the residual stress is taken into account. Hence, in further study, $\omega_0 = b/1000$.

4.1.3 Column length

Fig. 7 shows the load-displace relationships of columns with b/t of 40 and 60. Examination shows the responses of the two kinds of columns are similar except for the short and medium columns with b/t of 60. For sections with b/t of 40, the overall flexural buckling is in the majority, while for those with b/t of 60, the interaction of global and local buckling is observed.

According to the difference of the post-peak behavior, the responses of welded box columns with slender plate elements, as shown in Fig. 7(b), can be categorized into three types (Fig. 8).

Because of initial geometrical imperfections, from the beginning, flexural deformations, both overall and local occur. Along with an increasing loading, the two types of flexural deformations increase continuously and interact with each other. However, for a short column, the local deformation develops more quickly. The load-deformation curve consists of two parts: one ascending and the other descending. After reaching the peak load, it fails to carry the increased load owing to the excessive local buckling even under condition that the overall deformation is very small and the load-deformation response has a steep descending segment, as curve *a* shown in Fig. 8.

For a medium column, the overall and local deformations develop simultaneously and it is difficult to identify which one is more quickly. Similar to a short column, the load-deformation curve consists of ascending and descending portions (curve *b* in Fig. 8). However, after the maximum load, the curve decreases slowly, showing a higher post-peak strength reserve.

In the case of a long column, the overall flexural deformation increase more quickly, particularly after the onset of yielding, and the member exhibits a substantial post-peak reserve strength and good

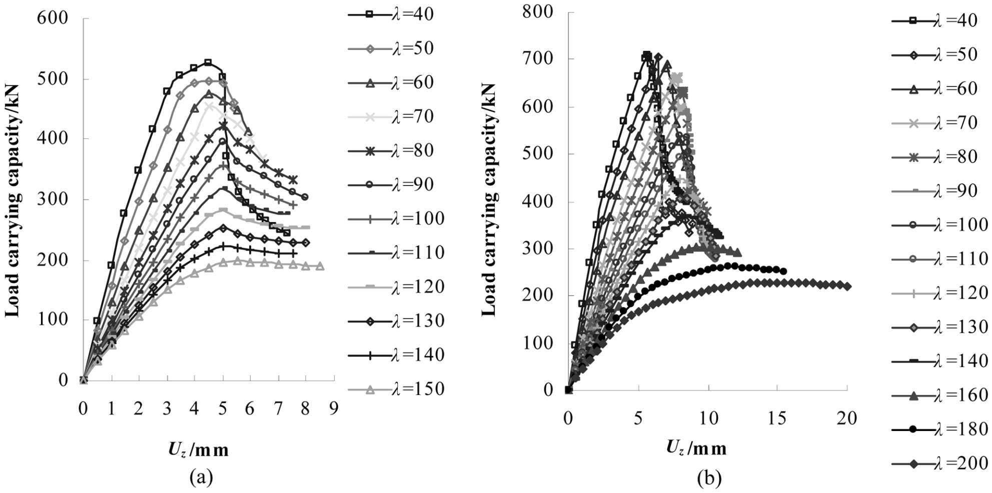

Fig. 7 Comparison of load-deformation responses (a) $b/t = 40$ (b) $b/t = 60$

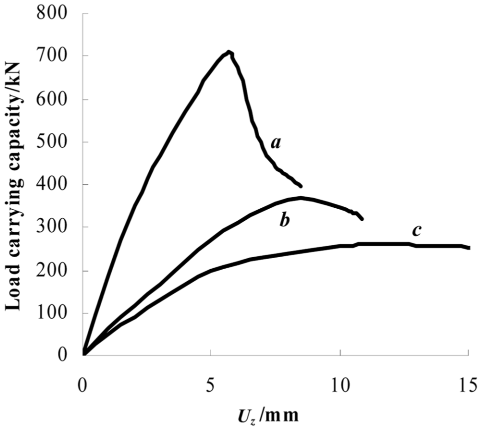

Fig. 8 Effect of column length

ductility, with an apparent horizontal segment on the load-deformation curve, such as the curve *c* shown in Fig. 8.

It is known that, from the above three cases, the longer a column, the better its ductility. Therefore, a square welded section whose width-to-thickness ratio exceeds the code limit is more suitable for a bracing, in which a larger slenderness ratio is expected.

4.1.4 Width-to-thickness ratio

Fig. 9 plots the ultimate load carrying capacity of the columns with different slenderness ratios and width-to-thickness ratios, one expressed in the overall stability factor φ (Fig. 9(a)), and the other in the ultimate strength (Fig. 9(b)). Also, the results calculated according to the Chinese code GB50017-2003 are shown in Fig. 9(a), and compared with the numerical results of column strengths for $b/t = 40$, 60, 70, 80, 100. It can be seen that on condition of the same slenderness ratio λ, the smaller the plate width-to-thickness ratio, the smaller the difference between the results obtained by using ANSYS and from

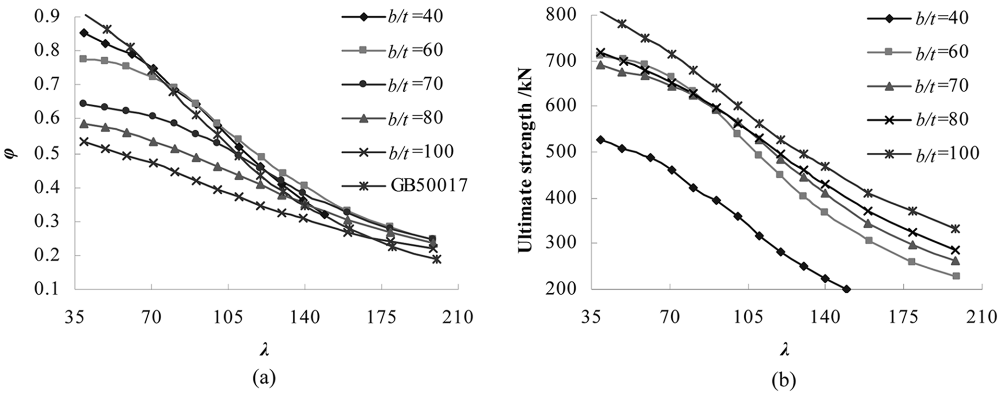

Fig.9 Effect of width-to-thickness ratio (a) φ-λ curves (b) Ultimate strength-λ curves

Chinese code GB50017-2003, and that on condition of the same width-to-thickness ratio, the longer the member, the closer the numerical result is to that calculated based on GB50017-2003. This just proves that the effect of plate width-to-thickness ratio mainly focuses on the behavior of the short and medium columns, rather than long columns. From Fig. 9(b),it can be known that the maximum load carrying capacity of columns with $b/t = 60$, 70, 80, 100 is much larger than that of columns with $b/t = 40$. However, for $b/t = 60,70,80,100$ columns, when slenderness ratio λ is less than 80, little increase in the ultimate carrying capacity is observed along with the increase of plate width-to-thickness ratio. Thus, the width-to-thickness ratio of the plate elements should not be too large, and the value of 100 is recommended as an upper bound.

4.2 Comparison between the numerical results and the calculated results using the effective width method

4.2.1 Chinese codes

At present, there are two basic design methods about how to take advantage of the post-buckling strength of the plate, the effective width method and direct strength method. The current Chinese design code GB 50017-2003 uses the former, and it is specified that only a width of $20t_w\sqrt{235/f_y}$ (t_w is the web thickness) on each side of the web should be considered effective in calculation of the strength and stability of members. This means that the effective width is only related to the thickness of the web, which is obviously not reasonable. The load-carrying capacity of an axially compressed member can be calculated according to the following formula

$$N_u = \varphi A_e f_y \tag{3}$$

where φ is the overall stability coefficient of an axially compressed member, given in the Appendix *C* of the Chinese code GB 50017-2003, and A_e is the effective cross-section area given in the other Chinese code GB 50018-2002 for design of cold-formed steel members.

A_e is defined more elaborately. Each plate element in a square box section column can be regarded as a stiffened plate, and its effective width-to-thickness ratio is calculated using the following formulas

when $\quad b/t \le 18\alpha\rho \qquad b_e/t = b_c/t \qquad$ (4a) when $18\alpha\rho < b/t < 38\alpha\rho$ $$b_e/t = \left[\sqrt{\frac{21.8\alpha\rho}{b/t}} - 0.1\right](b_c/t) \quad (4b)$$

when $b/t \geq 38\alpha\rho$ $$b_e/t = \frac{25\alpha\rho}{b/t} \cdot b_c/t \quad (4c)$$

Table 4 Comparison of the calculated results by the FEM and effective width method

b/t	60							70						
λ	P_u (kN)	N_u (kN)	P_n (kN)	N_{Rd} (kN)	P_u/N_u	P_u/P_n	P_u/N_{Rd}	P_u (kN)	N_u (kN)	P_n (kN)	N_{Rd} (kN)	P_u/N_u	P_u/P_n	P_u/N_{Rd}
40	710.76	622.66	656.58	647.10	1.14	1.08	1.10	690.18	665.49	682.61	675.51	1.04	1.01	1.02
50	703.98	601.74	636.16	622.25	1.17	1.11	1.13	675.64	643.23	663.74	651.81	1.05	1.02	1.04
60	689.78	577.46	611.99	594.79	1.19	1.13	1.16	665.89	617.38	641.35	625.92	1.08	1.04	1.06
70	663.08	542.33	577.33	555.85	1.22	1.15	1.19	646.06	579.96	609.06	589.56	1.11	1.06	1.10
80	633.57	508.39	546.62	520.75	1.25	1.16	1.22	623.58	543.81	580.36	556.84	1.15	1.07	1.12
90	589.86	471.85	513.97	482.69	1.25	1.15	1.22	593.07	504.86	549.58	521.08	1.17	1.08	1.14
100	539.05	438.70	479.87	442.95	1.23	1.12	1.22	564.44	469.51	517.14	483.05	1.20	1.09	1.17
110	493.92	402.74	444.92	403.22	1.23	1.11	1.22	526.09	431.16	483.63	444.09	1.22	1.09	1.18
120	448.13	369.13	409.57	365.09	1.21	1.09	1.23	485.73	395.29	449.40	405.69	1.23	1.08	1.20
130	404.41	338.05	374.42	329.68	1.20	1.08	1.23	446.16	362.11	415.11	369.11	1.23	1.07	1.21
140	368.04	311.05	339.89	297.56	1.18	1.08	1.24	409.23	333.28	380.95	335.20	1.23	1.07	1.22
160	304.97	251.77	274.18	243.42	1.21	1.11	1.25	345.77	285.82	315.01	276.66	1.21	1.10	1.25
180	260.28	204.84	217.48	201.21	1.27	1.20	1.29	297.15	238.99	253.65	229.99	1.24	1.17	1.29
200	228.11	170.55	176.64	168.38	1.34	1.29	1.35	262.6	198.98	206.02	193.19	1.32	1.27	1.36
b/t	80							100						
λ	P_u (kN)	N_u (kN)	P_n (kN)	N_{Rd} (kN)	P_u/N_u	P_u/P_n	P_u/N_{Rd}	P_u (kN)	N_u (kN)	P_n (kN)	N_{Rd} (kN)	P_u/N_u	P_u/P_n	P_u/N_{Rd}
40	717.26	697.78	702.55	697.43	1.03	1.02	1.03	808.22	697.78	731.16	729.52	1.16	1.11	1.11
50	700.39	681.36	685.06	674.78	1.03	1.02	1.04	780.18	681.36	716.06	708.72	1.15	1.09	1.10
60	680.62	653.69	664.27	650.27	1.04	1.02	1.05	749.42	662.10	698.00	686.58	1.13	1.07	1.09
70	653.15	614.21	634.15	616.17	1.06	1.03	1.06	713.14	633.80	671.75	656.28	1.13	1.06	1.09
80	626.88	576.06	607.18	585.62	1.09	1.03	1.07	677.4	605.97	648.00	629.45	1.12	1.05	1.08
90	595.77	534.95	578.16	552.11	1.11	1.03	1.08	639.55	575.39	622.27	600.06	1.11	1.03	1.07
100	563.66	497.62	547.45	516.09	1.13	1.03	1.09	600.36	547.04	594.81	568.16	1.10	1.01	1.06
110	529.86	457.10	515.41	478.52	1.16	1.03	1.11	563.26	503.22	565.82	534.16	1.12	1.00	1.05
120	496.89	419.19	482.57	440.66	1.19	1.03	1.13	528.99	461.72	535.85	498.81	1.15	0.99	1.06
130	462.57	384.11	449.29	403. 8	1.20	1.03	1.15	496.73	423.30	505.12	463.12	1.17	0.98	1.07
140	430.29	353.61	416.00	368.91	1.22	1.03	1.17	467.28	389.87	473.93	428.08	1.20	0.99	1.09
160	370.99	303.38	350.69	307.22	1.22	1.06	1.21	409.17	334.76	411.41	363.08	1.22	0.99	1.13
180	323.99	261.35	289.04	256.89	1.24	1.12	1.26	370.13	288.59	350.63	307.43	1.28	1.06	1.20
200	287.63	227.40	234.80	216.64	1.26	1.23	1.33	333.55	252.87	293.27	261.46	1.32	1.14	1.28

where b is the plate width, t the plate thickness, b_e the plate effective width, b_c the width of compressive part of the plate, and α and ρ are calculation coefficients. For a uniformly compressed plate element (as in the box section), then $\alpha = 1$ and $b_c = b$. The coefficient ρ is expressed as

$$\rho = \sqrt{\frac{205 k_1 k}{\sigma_1}} \tag{5}$$

in which k is the buckling coefficient, $k = 4$ for a long plate with all the edges simply supported; k_1 is the constraint factor of plate elements, $k_1 = 1$ in case there is no interaction between the adjacent plate elements; $\sigma_1 = \varphi f$, f being the design strength of steel.

By applying the above Eqs. (3)~(5), the maximum strength of the welded box-section columns, N_u, is calculated and listed in Table 4, in comparison with the numerical result, P_u. The thickness of the plate t=4mm when calculating these values. The ratios of P_u/N_u are also given in Table 4. The maximum, minimum and average values of P_u/N_u are 1.34, 1.03, and 1.18, respectively, and the standard deviation is 7.5%. The comparison shows that these design formulas, which are based on the effective width method,given in the Chinese code GB 50018-2002 are very conservative when used to calculate the ultimate strength of the welded box-section columns. Moreover, the end restraints of columns in the finite element model are treated as an ideal hinge, and in practice the end restraints are stronger, which results in higher column strengths.

4.2.2 American Standard ANSI/AISC 360-10

According to the American Standard ANSI/AISC 360-10, the nominal strength P_n of the compression members with slender elements shall be determined as follows

$$P_n = F_{cr} A \tag{6}$$

where A is the total cross-sectional area of a member, and F_{cr} the flexural buckling stress and determined by

$$\text{when} \quad \frac{KL}{r} \le 4.71\sqrt{\frac{E}{QF_y}} \qquad F_{cr} = Q\left[0.658^{\frac{QF_y}{F_e}}\right]F_y \tag{7a}$$

$$\text{when} \quad \frac{KL}{r} > 4.71\sqrt{\frac{E}{QF_y}} \qquad F_{cr} = 0.877 F_e \tag{7b}$$

where K is the effective length factor, L laterally unbraced length of the member, r governing radius of gyration, F_y steel yield strength, F_e the elastic critical buckling stress, and Q the reduction factor and $Q = Q_a$ for cross sections composed of only stiffened slender elements.

$$Q_a = \frac{A_e}{A} \tag{8}$$

where A_e is the effective cross-section area based on effective width b_e.

The effective width b_e is determined as follows

$$b_e = 1.92t\sqrt{\frac{E}{f_1}}\left[1-\frac{0.38}{(b/t)}\sqrt{\frac{E}{f_1}}\right] \le b \tag{9}$$

where $$f_1 = P_n / A_e \tag{10}$$

Strength calculation of a column according to Eqs. (6)~(10) requires iteration. In order to simplify this process, f_1 is taken equal to F_y. The calculated result, P_n, is listed in Table 4, and compared with the numerical result, P_u. The ratios of P_u/P_n vary from 0.98 to 1.29 with the average value of 1.08 and standard deviation of 6.7%. All these data show the numerical results agree well with the predictions in accordance with ANSI/AISC 360-10 except for the members with $b/t = 60$ and $\lambda = 180,200$, and for these members the ANSI/AISC 360-10 is slightly conservative estimate of column capacity. This may be caused by the simplification in the calculation.

4.2.3 Eurocode 3 EN1993-1

The section with large width-to-thickness ratio has to be designed as slender class-4 section in the latest Eurocode version EN 1993-1-1 and EN 1993-1-5. The buckling resistance of class-4 cross sections subjected to compression should be taken as

$$N_{Rd} = \chi A_{eff} f_y \tag{11}$$

where A_{eff} is the effective cross section in pure compression; χ is the reduction factor for the relevant buckling mode and it should be determined according to

$$\chi = \frac{1}{\Phi + \sqrt{\Phi^2 - \bar{\lambda}^2}} \le 1.0 \tag{12}$$

in which $$\Phi = 0.5[1 + \alpha_1(\bar{\lambda} - 0.2) + \bar{\lambda}^2] \tag{13}$$

$$\bar{\lambda} = \sqrt{\frac{A_{eff} f_y}{N_{cr}}} = \sqrt{\frac{A_{eff}}{A}} \cdot \frac{L_{cr}}{i\lambda_1} \tag{14}$$

where α_1 is an imperfection factor, for welded box sections, $\alpha_1 = 0.34$, L_{cr} the buckling length, i the radius of gyration, and λ_1 the Euler slenderness, $\lambda_1 = \pi\sqrt{E/f_y} = 93.9\sqrt{235/f_y}$.

The effective area of the compression zone of a plate with the gross cross-sectional area A_c should be obtained from

$$A_{c,eff} = \rho_1 A_c \tag{15}$$

where ρ_1 is the reduction factor for plate buckling and may be taken as following

$$\rho_1 = 1.0 \quad \text{for} \quad \bar{\lambda}_p \le 0.673 \tag{16}$$

$$\rho_1 = \frac{\bar{\lambda}_p - 0.055(3+\psi)}{\bar{\lambda}_p^2} \quad \text{for } \bar{\lambda}_p > 0.673\text{, where } (3+\psi) \ge 0 \tag{17}$$

where $\bar{\lambda}_p = \sqrt{f_y/\sigma_{cr}} = (b/t)/(28.4\varepsilon\sqrt{k_\sigma})$, ψ is the stress ration, $\varepsilon = 1$ for Q235 steel grades, k_σ is the buckling factor, and σ_{cr} the elastic critical plate buckling stress.

The buckling resistance, N_{Rd}, is obtained from Eqs. (11)~(17), and also compared with the numerical results, P_u, in Table 4. The ratios of P_u/N_{Rd} range from 1.02 to 1.36, and the average value and the standard deviation are 1.15, and 8.9%, respectively. Just like the Chinese code GB 50018-2002, the Eurocode 3 underestimates the capacities of welded box section columns over a wide range of slenderness ration.

4.3 Comparison between the numerical results and the calculated results using the direct strength method

The load-carrying capacity of a compression member can also be calculated using the direct strength method through the following formulas (AISI 2004)

$$\text{when} \quad \lambda_l \le 0.776 \qquad P_l = P_m \tag{18a}$$

$$\text{when} \quad \lambda_l > 0.776 \qquad P_l = \left[1 - 0.15\left(\frac{P_{cr,l}}{P_m}\right)^{0.4}\right]\left(\frac{P_{cr,l}}{P_m}\right)^{0.4} P_m \tag{18b}$$

$$\lambda_l = \sqrt{P_m/P_{cr,l}} \tag{19}$$

where P_l is the load-carrying capacity of a column calculated using the direct strength method; P_m is the overall stability capacity and is expressed as

$$P_m = \varphi A f_y \tag{20}$$

$P_{cr,l}$ is the local buckling load and is given by

$$P_{cr,l} = \sigma_{cr,l} A \tag{21}$$

in which $\sigma_{cr,l}$ is the critical stress of a plate under uniform compression, for a plate simply supported on four edges, it can be expressed as

$$\sigma_{cr,l} = \frac{4\pi^2 E}{12(1-v^2)}\left(\frac{t}{b}\right)^2 \tag{22}$$

The calculated results by Eqs. (18)~(22) are compared with the numerical results, as shown in Table 5. In this table, P_u represents the numerical result, P_{l1} the calculated result using the direct strength method. The values of P_{l1} correlate fairly well with those of P_u. The maximum, minimum, and average values of P_u/P_{l1} are 1.32, 0.94, and 1.07, respectively, and the standard deviation is 8.8%.

Eqs. (18a)~(18b) used for the design of cold-formed steel sections were modified by Kwon *et al.* (2007) and expressed as follows

$$\text{when} \quad \lambda_l \le 0.816 \qquad P_l = P_m \tag{23a}$$

Table 5 Comparison of the calculated results by the FEM and direct strength method (AISI 2004)

b/t	60			70			80			100		
λ	P_{l1} (P_{l2}) (kN)	P_u (kN)	P_u/P_{l1} (P_u/P_{l2})	P_{l1} (P_{l2}) (kN)	P_u (kN)	P_u/P_{l1} (P_u/P_{l2})	P_{l1} (P_{l2}) (kN)	P_u (kN)	P_u/P_{l1} (P_u/P_{l2})	P_{l1} (P_{l2}) (kN)	P_u (kN)	P_u/P_{l1} (P_u/P_{l2})
40	698.31 (696.85)	710.76	1.018 (1.020)	732.99 (712.46)	690.18	0.942 (0.969)	763.05 (724.13)	717.26	0.940 (0.991)	813.28 (740.40)	808.22	0.994 (1.092)
50	676.34 (677.55)	703.98	1.041 (1.039)	710.32 (693.26)	675.64	0.951 (0.975)	739.62 (704.96)	700.39	0.947 (0.994)	788.70 (721.28)	780.18	0.989 (1.082)
60	650.74 (655.01)	689.78	1.060 (1.053)	683.82 (670.72)	665.89	0.974 (0.993)	712.33 (682.47)	680.62	0.955 (0.997)	760.04 (698.84)	749.42	0.986 (1.072)
70	613.49 (621.82)	663.08	1.081 (1.066)	645.22 (637.62)	646.06	1.001 (1.013)	672.62 (649.44)	653.15	0.971 (1.006)	718.29 (665.89)	713.14	0.993 (1.071)
80	577.24 (589.22)	633.57	1.098 (1.075)	607.69 (605.07)	623.58	1.026 (1.031)	633.88 (616.95)	626.88	0.989 (1.016)	677.64 (633.47)	677.4	0.999 (1.069)
90	537.90 (553.36)	589.86	1.097 (1.066)	566.90 (569.31)	593.07	1.046 (1.042)	591.89 (581.24)	595.77	1.007 (1.025)	633.47 (597.86)	639.55	1.010 (1.070)
100	501.88 (509.18)	539.05	1.074 (1.059)	529.58 (536.17)	564.44	1.066 (1.053)	553.39 (548.16)	563.66	1.019 (1.028)	593.01 (564.85)	600.36	1.012 (1.063)
110	452.30	493.92	1.092	488.71 (499.39)	526.09	1.076 (1.053)	511.26 (511.43)	529.86	1.036 (1.036)	548.67 (528.22)	563.26	1.027 (1.066)
120	400.92	448.13	1.118	450.10 (464.09)	485.73	1.079 (1.047)	471.42 (476.21)	496.89	1.054 (1.043)	506.75 (493.09)	528.99	1.044 (1.073)
130	355.05	404.41	1.139	414.00 (413.25)	446.16	1.078 (1.080)	434.17 (442.81)	462.57	1.065 (1.045)	467.56 (459.77)	496.73	1.062 (1.080)
140	316.52	368.04	1.163	368.40	409.23	1.111	401.47 (413.04)	430.29	1.072 (1.042)	433.12 (430.07)	467.28	1.079 (1.087)
160	255.97	304.97	1.191	297.93	345.77	1.161	339.89	370.99	1.092	375.58 (379.48)	409.17	1.089 (1.078)
180	208.26	260.28	1.250	242.40	297.15	1.226	276.54	323.99	1.172	326.51 (335.22)	370.13	1.134 (1.104)
200	173.40	228.11	1.316	201.82	262.6	1.301	230.25	287.63	1.249	287.10	333.55	1.162

$$\text{when } \lambda_l > 0.816 \quad P_l = \left[1 - 0.15\left(\frac{P_{cr,l}}{P_m}\right)^{0.5}\right]\left(\frac{P_{cr,l}}{P_m}\right)^{0.5} P_m \tag{23b}$$

The modified direct strength formulas (23a) and (23b), proved to be capable of predicting the ultimate strength of welded H and channel section columns (Kwon *et al.* 2007), are also used for welded box sections and the calculation result, P_{l2}, is given in parentheses in Table 5, where only one is listed when the results calculated using two methods are same. Examination shows that for $b/t = 60$ sections it seems difficult to determine which one, direct strength method or modified direct strength method, is more suitable for the welded box sections only from the values in Table 5. However, for $b/t = 70$, 80 and 100, it is obvious that the numerical results coincide well with the calculation results by the modified direct strength method. Therefore, the modified direct strength method is a reasonable predictor of strength over a wide range of width-to-thickness ratio and should be recommended for welded box sections with slender elements.

5. Conclusions

A double nonlinear finite element model taking account of both the geometric and material imperfections is developed by using the ANSYS program. The interaction of local and overall buckling and the ultimate capacity of welded thin-wall box steel columns with high width-to-thickness ratios (i.e., $b/t = 60$, 70, 80, 100) are analyzed by the proposed model. Comparisons between the numerical results and the calculated results using the effective width (provided in the Chinese code GB50018-2002, American standard ANSI/AISC 360-10 and Eurocode 3 EN 1993-1) and direct strength method, are also performed. The following conclusions can be drawn from this study.

(1) The finite element model proposed in this paper can simulate the nonlinear buckling behavior of welded box section columns under axial compression very well.

(2) The plate width-to-thickness ratio of welded square box axially compressed members can be enlarged to 100 to take advantage of the post-buckling strength of plate elements, thus enhancing the column strength.

(3) There are large differences between the numerical results and the calculation results according to the Chinese code GB50018-2002 and Eurocode 3 EN 1993-1, and the two standards are very conservative. At the same time, the study also shows the American standard ANSI/AISC 360-10 provides a better prediction of the ultimate capacity of welded square box columns except for lower width-to-thickness ratio $b/t = 60$ and for these members it is slightly conservative.

(4) The numerical results are in good agreement with those from the direct strength method and modified direct strength method.

(5) The modified direct strength method, rather than direct strength method, is more suitable for the welded square box columns with high width-to-thickness ratio, thus it is suggested that this method should be adopted when revising the Chinese code.

Acknowledgments

The research reported in the paper is the project supported by the Research Foundation of Education Bureau of Shaanxi Province, China (Grant No. 11JK0950), and the project supported by Start-Up Fund for Outstanding Incoming Researchers of Xi'an University of Architecture and Technology, China (Grant No. RC0813). Their financial support is highly appreciated. Thanks to Professor Shao-Fan Chen for his help in providing valuable advice about modifying this paper.

References

American Iron and Steel Institute (AISI), "Supplement 2004 to the North American specifications for the design of cold-formed steel structural members", Washington (DC, USA); 2004.

ANSI/ AISC 360-10, "Specification for Structural Steel Buildings" , An American National Standard.

Becque, J., Lecce, M. and Rasmussen, Kim J. R. (2008), "The direct strength method for stainless steel compression members", *J. Constr. Steel Res.*, **64**(11), 1231-1238.

Becque, J. and Rasmussen, Kim J. R. (2009), "A numerical investigation of local-overall interaction buckling of stainless steel lipped channel columns", *J. Constr. Steel Res.*, **65**(8-9), 1685-1693.

Chen, S. F. (1992), *Steel structures*, Beijing, China. (in chinese)

de Miranda Batista, E. (2009), "Local–global buckling interaction procedures for the design of cold-formed

columns: Effective width and direct method integrated approach", *Thin-Walled Struct.*, **47**(11), 1218-1231.
Degée, H., Detzel, A. and Kuhlmann, U. (2008), "Interaction of global and local buckling in welded RHS compression members", *J. Constr. Steel Res.*, **64**(8-9), 755-765.
EN 1993-1-1: 2005, "Design of steel structures-Part 1-1: General rules and rules for buildings," 2005.
EN 1993-1-5: 2006, "Design of steel structures-Part 1-5: Plated structural elements," 2006.
Fan, Z., Fan, X. W. and Liu, X. M.(2006), "Design method for welded thin-wall box components", *Prog. Steel Build. Struct.*, **8**(3), 34-40.(in Chinese)
GB 50017-2003, "Code for design of steel structures", National Standard of the People's Republic of China.
GB 50018-2002, "Technical code of cold-formed thin-wall steel structures", National Standard of the People's Republic of China. (in chinese)
Guo,Y. L. (1992), "Ultimate load behavior of welded thin-walled stub columns under combined loading of axial compression and bending", *Comput. Struct.*, **42**(4), 591-597.
Kwon, Y. B., Kimand, N. G. and Hancock, G. J. (2007), "Compression tests of welded section columns undergoing buckling interaction", *J. Constr. Steel Res.*, **63**(12), 1590-1602.
Pircher, M., O'Shea, M. D. and Bridge, R. Q. (2002), "The influence of the fabrication process on the buckling of thin-walled steel box sections", *Thin-Walled Struct.*, **40**(2), 109-123.
Rusch, A. and Lindner, J. (2001), "Remarks to the direct strength method", *Thin-Walled Struct.*, **39**(9), 807-820.
Schafer, B. W. (2008), "Review: The direct strength method of cold-formed steel member design", *J. Constr. Steel Res.*, **64**(7-8), 766-778.
Sputo, T. and Tovar, J. (2005), "Application of direct strength method to axially loaded perforated cold-formed steel studs: Longwave buckling", *Thin-Walled Struct.*, **43**(12), 1852-1881.
Swanson Analysis Systems Inc (2004), *Ansys Reference Manual*, version 8.1.
Tovar, J. and Sputo,T. (2005), "Application of direct strength method to axially loaded perforated cold-formed steel studs: Distortional and local buckling", *Thin-Walled Struct.*, **43**(12), 1882-1912.
Usami, T. and Fukumoto,Y. (1982), "Local and overall buckling of welded box columns", *J. Struct. Div.*, **108**(ST3), 525-542.
Usami, T. and Fukumot,Y. (1984), "Welded box compression members",*J. Struct. Eng.*, **110**(10), 2457-2471.
Yang, N., Long, L. H. and Yang Q. S. (2007), " The interactive-buckling analysis of tapered H-section steel beams with thin web", *Ind. Constr.*, **37**(1), 96-100. (in chinese)
Yu, C. and Schafer, B. W. (2007), "Simulation of cold-formed steel beams in local and distortional buckling with applications to the direct strength method", *J. Constr. Steel Res.*, **63**(5), 581-590.
Zhu, J. H. and Young, B. (2006), "Aluminum alloy tubular columnsPart II: Parametric study and design using direct strength method", *Thin-Walled Struct.*, **44**(9), 969-985.

CC

Nomenclature

A, A_c	cross-section area
A_e, A_{eff}, $A_{c,eff}$	effective cross-section area
b	plate width
b_c	plate compressive zone width
b_e	plate effective width
c	distribution length of tensile residual stresses
E	Young's modulus
E_t, E_{t1}, E_{t2}	tangent modulus
f	steel design strength
f_1	section stress, $f_1 = P_u/A_e$
f_y, F_y	steel yield strength
F_{cr}	flexural buckling stress
F_e	elastic critical buckling stress
h	cross-section depth

h_0	distance between the centre lines of the two opposite plates
k	buckling coefficient
k_1	constraint factor of plate elements
K	effective length factor
l	column length
L, L_{cr}	laterally unbraced length of the member
m	buckling half-wave number along the axial direction (z–direction)
N_{Rd}	buckling resistance according to EN 1993-1
N_u	load-carrying capacity according to GB 50018-2002
P_u	numerical result
$P_{cr,l}$	critical local buckling load
P_l	column strength
P_{l1}	load-carrying capacity calculated using the direct strength method
P_{l2}	load-carrying capacity calculated using the modified direct strength method
P_m	overall stability capacity of a column
P_n	nominal strength according to ANSI/AISC 360-10
Q, Q_a	reduction factor
r, i	governing radius of gyration
t	plate thickness
t_w	web thickness
U_x, U_y, U_z	translation in x, y, and z direction
x, y, z	coordinate axis
λ	slenderness ratio
$\bar{\lambda}$	non-dimensional global slenderness
$\bar{\lambda}_p$	non-dimensional plate slenderness
λ_1	Euler slenderness ratio
λ_l	a parameter, and $\lambda_l = \sqrt{P_m/P_{cr,l}}$
φ, φ_1, φ_2	overall stability coefficient of an axially compressed member
α, ρ, Φ	calculation coefficient
α_1	imperfection factor
ρ_1	reduction factor for plate buckling
σ_1	a parameter, and $\sigma_1 = \varphi f$
σ_{rc}	compressive residual stress
$\sigma_{cr,l}$, σ_{cr}	critical buckling stress of a plate
ω	plate local initial deflection
ω_0	amplitude of local buckling, and $\omega_0 = b/1000$
ν	Poisson's ratio
χ	the reduction factor for the relevant buckling mode
ψ	stress ration